Encapsulation of Poly(3-hexylthiophene) J-Aggregate Nanofibers with an Amphiphilic Block Copolymer

Jian Gao,[†] Amanda Kamps,[‡] So-Jung Park,[‡] John K. Grey[†*]

[†]Department of Chemistry and Chemical Biology, University of New Mexico, Albuquerque, NM 87131

[‡]Department of Chemistry, University of Pennsylvania, Philadelphia, PA 19104

* email: jkgrey@unm.edu

Supporting Information

Structural stability of J-aggregate NF's

P3HT NF samples were prepared using different solvents that select either H-aggregate type NF's (anisole) or J-aggregate type (toluene). TEM imaging was used to compare structural attributes of both NF's to understand differences in packing characteristics. This information is useful for understanding how encapsulation by the BCP affects chain conformations and packing.

Fig. S1 shows TEM images of NF samples prepared from anisole (a) and toluene (b,c). Typically, anisole assembled samples show widths of ~20 nm whereas toluene NFs have larger widths of ~40 nm. These results corroborate the previously proposed structural attributes of NF

J-aggregates whereby P3HT chains are much more elongated than in H-aggregates thus giving rise to increased intra-chain order. In some cases, toluene assembled NFs show both H- and J-type features based on TEM images and optical spectra. This feature most commonly arises in aged samples or when temperatures are not controlled properly and can also be observed in absorption spectra.

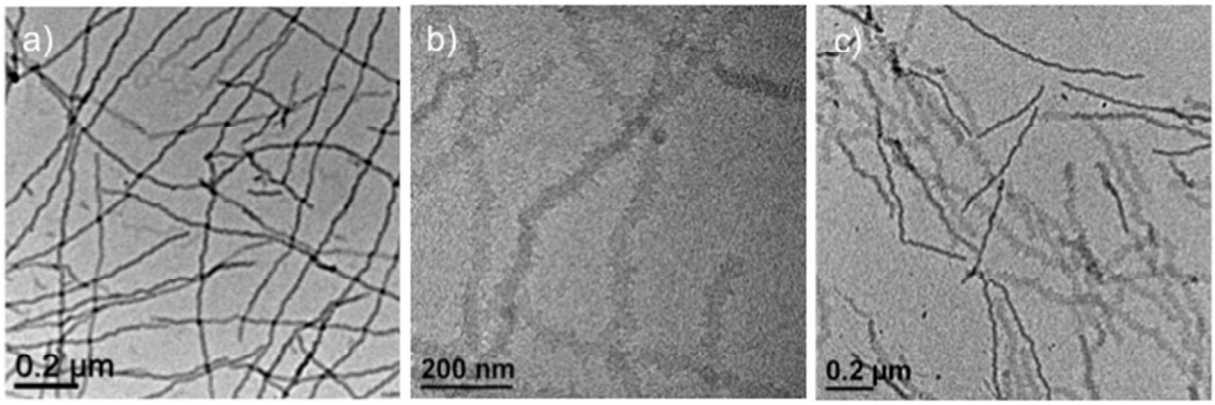

Figure S1. TEM images of pristine a) H-aggregate NF's, made from anisole solution and b) J-aggregate NF's, made from toluene solution. c) H- and J-aggregate NF's mixture in toluene NF's.

We also test the structural stabilities of the NFs by sonication. Fig. S2 compares J-aggregate NF aspect ratios before (a) and after (b) sonication treatments in solution dispersions. Interestingly, NFs retain J- aggregate character after sonication albeit with smaller aspect ratios. From this result, we expect the stability of the NF structure is suitable for encapsulation studies since changes in optical spectra should reflect interaction of the BCP coating and not degradation processes.

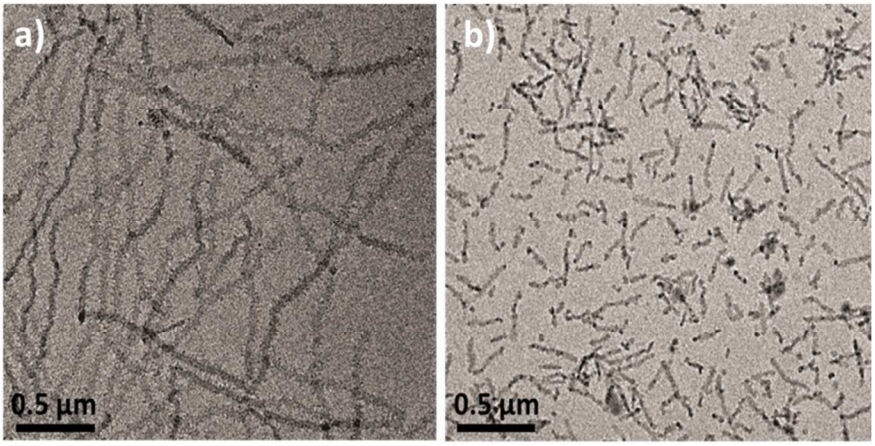

Figure S2. TEM images of toluene NF's a) before sonication and b) after sonication.

Raman overtones

Encapsulated NF Raman spectra display an overtone of the C=C mode appears at ~2900 cm^{-1} and a combination band corresponding to the C=C and C-C (~1380 cm^{-1}) modes at ~2840 cm^{-1}. Fundamentals of C-H stretches are also expected in this region (~2900-3000 cm^{-1}) that can potentially interfere with overtones. Fig. S3 compares IR and resonant Raman spectra of encapsulated and pristine samples which show little energetic overlap or similarity in intensity patterns as the overtone-combination band features.

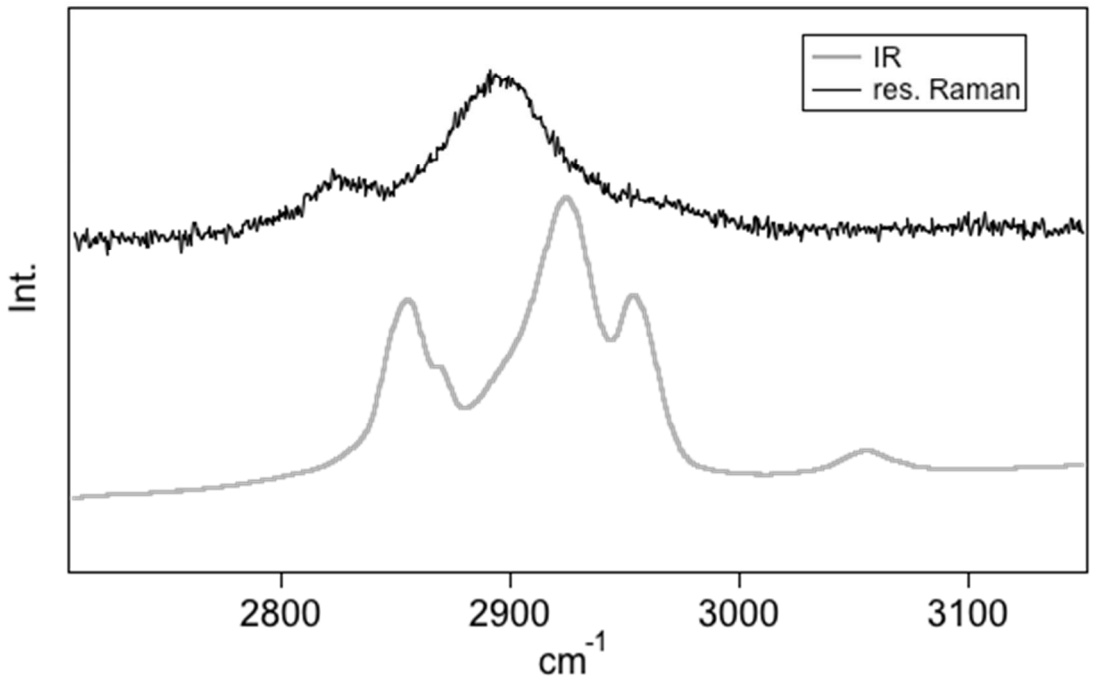

Figure S3. IR spectra (gray) and the Raman spectra (black) for BCP encapsulated NF's.

Raman spectra of NF's were also measured off-resonance with 782 nm light and compared to lineshapes generated under resonance conditions which are shown in Fig. S4. Inspection of the first overtone region reveals very low intensities for the off-resonance condition which is expected due to the small enhancement factors because the excitation wavelength is far from the absorption transition onset.

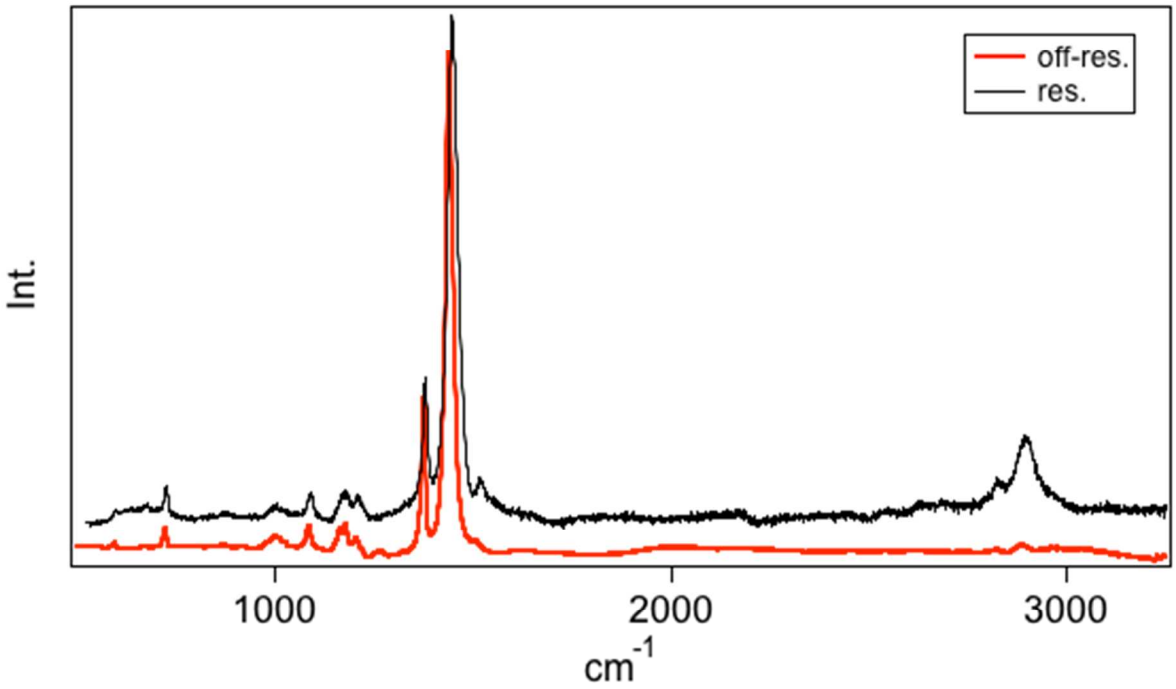

Figure S4. IR spectra (gray) and the Raman spectra (black) for BCP encapsulated NF's.

Understanding the contribution of BCP to PL and Raman

BCP has very low emission efficiency in water and methanol compared with that in dichloromethane (DCM), which help sort out its contributions in the emission spectra of the encapsulated NFs in water and methanol. BCP can be dispersed in dichloromethane (DCM) where both polymer blocks are soluble. In water and methanol, the BCP can organize into supramolecular assemblies as evidenced by the redshift and the appearance of the vibronic structure in the UV-vis spectra. The efficient PL quenching of BCP in water and methanol is also indicative of tightly packed chains and strong interchain coupling in the polymer assemblies. Since the PL is weak for the BCP and we can treat the PL for the encapsulated NFs is mainly from the P3HT NFs.

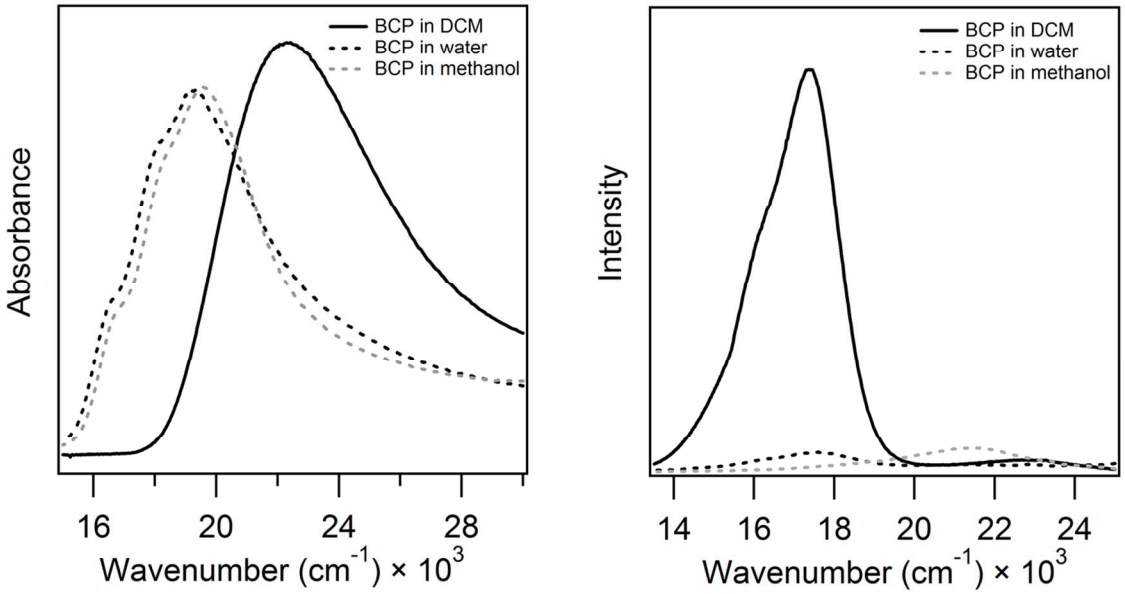

Figure S5. UV (left) and PL (right) for BCP in dichloromethane (black), water (black dashed) and methanol (grey dashed) at same concentrations.

In order to confirm that the BCP has little contribution to the emission and the Raman spectra for the encapsulated NFs, we compare both emission and Raman spectra for BCP and encapsulated NFs under the same conditions. We find the PL and Raman intensities of BCP is much lower than that of the encapsulated NFs (for samples from water and methanol).

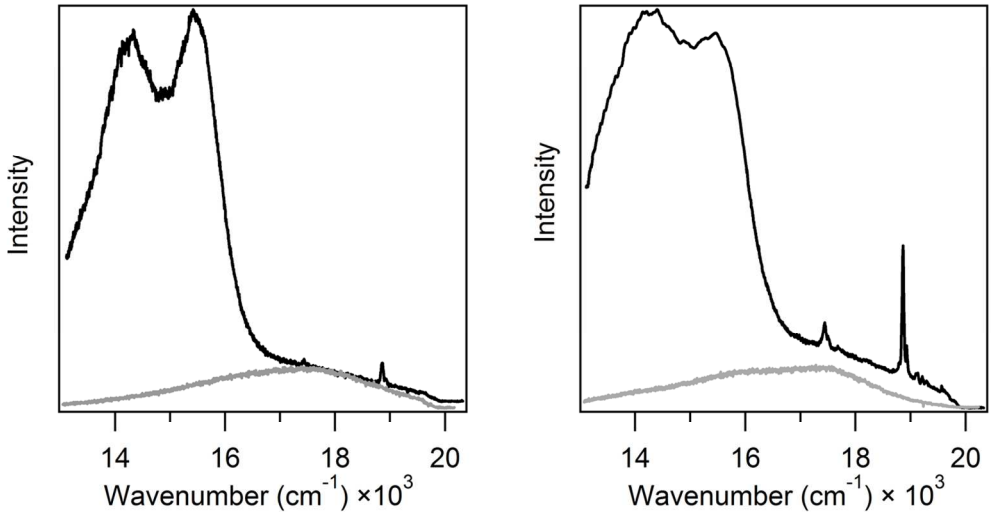

Figure S6. PL for BCP bulk film (grey) made from water solution (left) and methanol solution (right). In order to compare the relative intensity of the pure BCP and encapsulated NF's (black). Note: Raman peaks are discernible on the PL lineshapes of the encapsulated NF's indicating similar cross-sections.

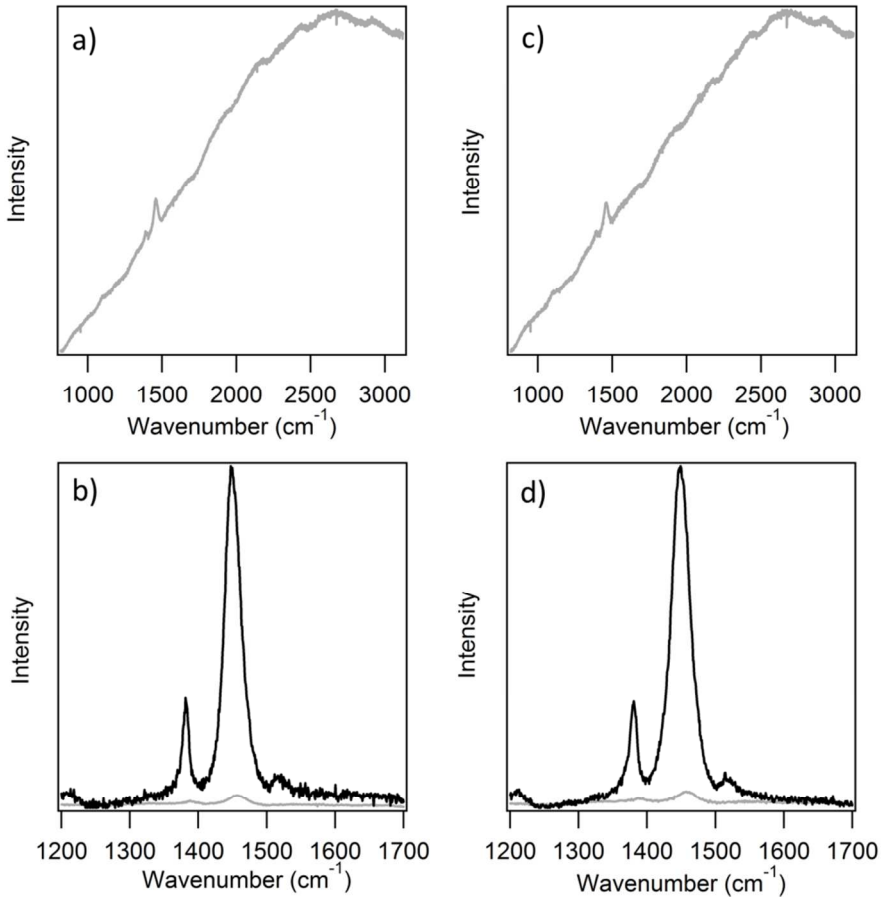

Figure S7. Comparison for the Raman spectra of BCP (gray) with the encapsulated NFs (black), a) and b) for BCP bulk film from water solution, c) and d) for BCP bulk film from methanol solutions.

From Fig. S7, Raman from BCP films is mostly obscured by background PL. The PL lineshape characteristics are also similar to those found from single particle imaging studies (see Fig. 4, main text). The Raman signal from pure BCP is mostly obscured by the PL signal and much weaker than that of encapsulated NFs (~20×). There are also ~15 cm^{-1} blue shifts of the dominant C=C mode in the BCP samples indicating that they are largely in the amorphous or, unaggregated, state.